

Light-induced D diffusion measurements in hydrogenated amorphous silicon: Testing H metastability models

Howard M. Branz and Sally Asher

National Renewable Energy Laboratory, Golden, Colorado 80401

Helena Gleskova and Sigurd Wagner

Department of Electrical Engineering, Princeton University, Princeton, New Jersey 08544

(Received 8 January 1998; revised manuscript received 16 September 1998)

We measure light-induced D tracer diffusion in hydrogenated amorphous silicon samples under conditions at which thermal diffusion is negligible. Under high-intensity (9 W cm^{-2}), red-light soaking at $135 \text{ }^\circ\text{C}$, the D diffusion coefficient is $D_D = 1.3 \times 10^{-18} \text{ cm}^2 \text{ s}^{-1}$ and the rate of D emission from Si-D to transport is $3.5 \times 10^{-5} \text{ s}^{-1}$. We also find an upper bound of $D_D = 3 \times 10^{-20} \text{ cm}^2 \text{ s}^{-1}$, the light-induced diffusion coefficient at $65 \text{ }^\circ\text{C}$. Previous experiments had revealed only ‘‘light-enhanced’’ diffusion between from 200 to $300 \text{ }^\circ\text{C}$, a regime in which thermal diffusion is also significant. Our $135 \text{ }^\circ\text{C}$ result extends the range of the 0.9-eV activation energy for this diffusion; our $65 \text{ }^\circ\text{C}$ upper bound is consistent with the extrapolation of the higher temperature data. We also measure metastable defect creation at 65 and $135 \text{ }^\circ\text{C}$ to test models of light-induced metastability that involve emission of H from Si-H bonds to an H transport level. This class of models can be limited, but not excluded, by our data. The H emission parameter of the H collision model of metastability is also estimated. [S0163-1829(99)09407-2]

I. INTRODUCTION

Excess carriers in hydrogenated amorphous silicon (*a*-Si:H) cause a dramatic increase in the density of deleterious threefold-coordinated Si, dangling bond (DB) defects. This ‘‘Staebler-Wronski’’ (SW) effect¹ is an important problem in the physics of amorphous semiconductors both because of its inherent interest and because the effect has handicapped the application of *a*-Si:H as a low-cost thin-film semiconductor. Numerous hydrogen-related models of the SW effect have been proposed.²⁻⁹ Most recently, one of us has proposed a quantitative microscopic model explicitly involving long-range H diffusion¹⁰ that is supported by microscopic theoretical calculations,¹¹ and is consistent with the light-induced creation of DB’s at 4.2 K .¹²

Recent electron spin resonance (ESR) data cannot be reconciled with the many models of the SW effect involving only local motion of H during DB formation. Such local models leave a H atom in close proximity to the light-induced DB. The DB should, therefore, show a H hyperfine signature that is not seen by ESR studies.^{13,14} Therefore, among the H models of the SW effect, only long-range H diffusion models must be seriously considered.

Light-enhanced D effusion from *a*-Si:D:F samples between 400 and $600 \text{ }^\circ\text{C}$ was discovered by Weil, Busso, and Beyer.¹⁵ Further D tracer^{7,16} and hydrogen¹⁷ diffusion experiments revealed a diffusion enhancement between 200 and $300 \text{ }^\circ\text{C}$. Santos and Johnson¹⁸ demonstrated that excess carriers cause the enhanced diffusion, a rather compelling parallel with the SW effect. However, these measurements of ‘‘light-enhanced diffusion’’ were all made at temperatures so high that dark D diffusion was also observed. Further, defect thermal annealing renders SW defect creation kinetics impossible to measure above about $150 \text{ }^\circ\text{C}$. Therefore, quantitative comparison of H diffusion rates with the SW defect

creation rates have previously been impossible.

In this paper, we report parallel measurements of light-induced D tracer diffusion and metastable DB creation in *a*-Si:H at 135 and $65 \text{ }^\circ\text{C}$. We measure the D emission rate to transport at $135 \text{ }^\circ\text{C}$ and place an upper bound on D diffusion at $65 \text{ }^\circ\text{C}$. Our $135 \text{ }^\circ\text{C}$ result clearly demonstrates ‘‘light-induced’’ (rather than ‘‘light-enhanced’’) D diffusion in *a*-Si:H. We use our results to test and constrain the many models of SW defect creation involving light-induced H diffusion.⁵⁻¹¹

II. EXPERIMENTAL AND FITTING PROCEDURES

A. Tracer diffusion

Tracer-diffusion measurements are made on *a*-Si:H/*a*-Si:H:D/*a*-Si:H sandwich structures deposited on doped crystalline-Si substrates at $230 \text{ }^\circ\text{C}$. In the National Renewable Energy Laboratory deposition system, we can rapidly switch process gas flow between the deposition chamber and a bypass line that flows directly into the vacuum pump. The top and bottom layers are grown by plasma-enhanced chemical-vapor deposition (PECVD) at about $2 \text{ } \text{Å/s}$ from SiH_4 diluted with an equal flow of H_2 . To deposit these *a*-Si:H layers, we flow H_2 and SiH_4 to the chamber but flow D_2 through the bypass line. To deposit the PECVD *a*-Si:H:D layer, we simultaneously switch the H_2 flow to the bypass and the D_2 flow to the chamber. In our PECVD chamber, near complete gas exchange occurs in approximately 10 s ($20 \text{ } \text{Å}$ of growth). To minimize D diffusion at this stage of the experiment, the two upper layers are kept thin ($\sim 600 \text{ } \text{Å}$) and we cool the sample immediately after growth. Secondary-ion-mass spectrometry (SIMS) shows that about 2% of all H in the layer (roughly 10 at. %) is substituted by D, meaning the D content is about 0.2 at. %. Films made from both of these gas mixtures in this reactor are device quality.¹⁶

We light soak the sandwich structure with 9 W cm^{-2} of uniformly absorbed light from a defocused continuous-wave Kr-ion laser (wavelengths of 676.4 and 647.1 nm). Half the sample is painted with colloidal black-graphite suspension to serve as a dark control with identical thermal history.¹⁶ The rate of photon absorption (electron-hole pair generation) at the deuterated layer is roughly $G=10^{23} \text{ cm}^{-3} \text{ s}^{-1}$. The sample temperature is maintained during illumination by a Peltier heater/cooler at constant voltage. To avoid shadowing the SIMS analysis region with a thermocouple, the temperature during laser-light soaking is not measured directly. Rather, temperature is determined by careful calibration of the voltage applied to the Peltier element against the temperature of a similar film, using a miniature thermocouple and the same Kr laser illumination. The calibration film is on glass but is pressed to *c*-Si that is in thermal-paste contact with the Peltier cooler. The miniature thermocouple is embedded in the thermal paste.

We measure D and O concentration profiles versus depth in the control and light-soaked regions by SIMS using negative secondary ions produced by 14-keV Cs^+ bombardment of the sample. Absolute D concentrations, accurate to within $\pm 30\%$, are obtained from a crystalline Si standard implanted with a dose of 10^{14} cm^{-2} D ions. Absolute depth scales are set by stylus profilometry of the SIMS craters. We use the upper edge (i.e., the edge closer to the free surface) of the D profiles for all the analyses reported here. The upper edge of as-grown profiles have a measured exponential decay length of $27 \pm 3 \text{ \AA}$, mainly due to residual D_2 in the deposition chamber during growth of the top layer. SIMS-induced propulsion of D into the bottom *a*-Si:H layer combines with annealing during sample deposition to broaden the lower edge of the D profiles considerably.

We study D diffusion by subjecting pieces of a single sandwich structure to different dark and illuminated anneal treatments. Precise, relative, depth scales between different profiles are established with the aid of a slight oxygen contamination in the *a*-Si:H:D layer. The O originates in impure D_2 gas. Because oxygen diffusion is always found to be negligible, we set final depth scales by rescaling the crater depth slightly to precisely match the O profiles before and after annealing. The absolute magnitude of the rescaling is within the measurement error of the stylus profilometer used to measure the SIMS crater. After the O-based depth matching, we study the corresponding D profiles without any further rescaling of the depth. While absolute depth scaling is not improved by this procedure, comparison of different scans can be very accurate. For example, the edges of as-grown D profiles taken from different craters on the same sample align within about 10 \AA . Results reported below suggest a corresponding detection limit of about 10 \AA on the broadening of profiles.

B. Tracer profile fits

In the long-time diffusion regime,¹⁹ we fit the logarithm of the upper (left) edge of the measured D profile $C(x)$, to the logarithm of the ideal concentration profile,

$$C(x) = A/2 \operatorname{erfc}\{(x - x_0)/\sqrt{(4D_D t)}\}, \quad (1)$$

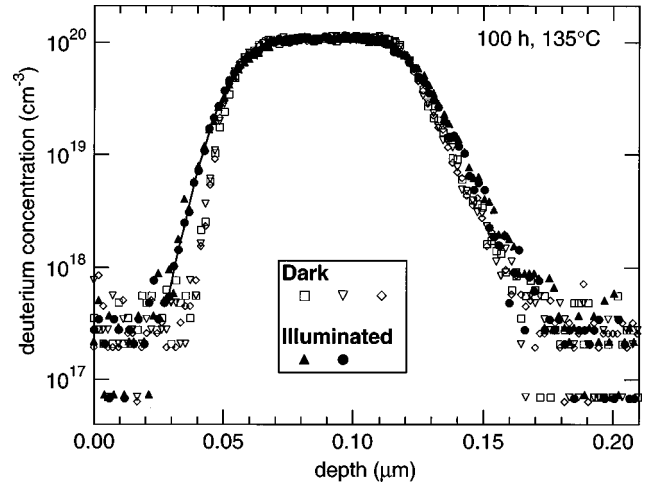


FIG. 1. D depth profiles from dark (open symbols) and laser-illuminated (filled symbols) regions of a sandwich sample after 100 h at $135 \text{ }^\circ\text{C}$. Profiles from several SIMS craters in each region are shown. Best-fit curve of Eq. (1) to one illuminated profile (solid circles) is also shown.

for diffusion from a semi-infinite region of initial concentration A . Here, x is the depth, x_0 is the initial step depth, D_D is the deuterium diffusion coefficient, and t is the anneal time. In the early- and intermediate-time regimes,¹⁹ we fit the logarithm of the upper wing of $C(x)$ to the logarithm of an exponential decay

$$C(x) = B \exp\{(x - x_0)/\lambda_m\}, \quad (2)$$

where B is the amplitude of the exponential wing and λ_m is the measured decay length. We normally take the logarithm of the data and the fitting equations to give nearly equal weight to all points in the fit.

C. Defect density

At intervals during the early stages of light soaking, we measure the room-temperature subgap optical absorption of a second sandwich structure deposited simultaneously on Corning 7059 glass. The absorption is measured by the constant photocurrent method (CPM) and converted to defect density as described elsewhere.²⁰ Because of the extremely high-intensity illumination and the low thermal-conductivity glass substrate, we were unable to control the sample temperature well during the first seconds of illumination. The temperature of a calibration sample grown on a Ni resistance “thermometer” reached its setpoint about 10 s after the start of laser illumination. In all cases, the sample temperature was actually ramped, but we report an average temperature of the light soaking. The “ $65 \text{ }^\circ\text{C}$ soak” began from $10 \text{ }^\circ\text{C}$ and rose to $63 \text{ }^\circ\text{C}$ at 1.5 s and $95 \text{ }^\circ\text{C}$ after 10 s. The “ $135 \text{ }^\circ\text{C}$ ” soak began from $73 \text{ }^\circ\text{C}$ and rose to $156 \text{ }^\circ\text{C}$ at 5 s.

III. RESULTS

Figure 1 shows measured D depth profiles from two SIMS craters after 100 h light soaking of a sandwich structure at $135 \text{ }^\circ\text{C}$. For comparison, three dark profiles from the black-painted region of the sample are also shown. The dark profiles are unchanged from a control, unannealed sample.

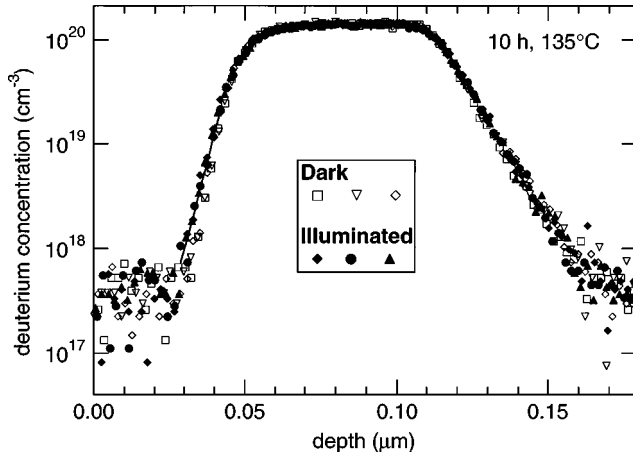


FIG. 2. D depth profiles from dark (hollow symbols) and laser-illuminated (filled symbols) regions of a sandwich sample after 10 h at 135 °C. Profiles from several SIMS craters in each region are shown. The solid curve is a best-fit curve of one illuminated profile (solid circles) to Eq. (2).

The illuminated profiles are fit well by Eq. (1), as shown by the fit curve in Fig. 1. The best-fit light-induced diffusion coefficient is $D_D = 1.3 \times 10^{-18} \text{ cm}^2 \text{ s}^{-1}$.

Figure 2 shows D profiles from three SIMS craters after 10 h light soaking of a sandwich structure at 135 °C. For comparison, three dark profiles from the sample are also shown. The dark profiles are unchanged from a control, unannealed sample. The upper (left) edge of the illuminated profiles are broadened measurably and are well fit by Eq. 2, as shown. The broadening is from a characteristic decay length of $27 \pm 3 \text{ \AA}$ for the dark profile to $\lambda_m = 39 \pm 3 \text{ \AA}$ in the illuminated profile. 2 h light soaking at 135 °C revealed no measurable difference between the dark, illuminated, and control (unannealed) D profiles.

Figure 3 shows comparable data for 120 h illumination at 65 °C. Neither dark nor light-enhanced diffusion are observable. We calculated an upper bound to the diffusion coefficient by smoothing the measured as-grown profile and then using it as the initial condition for an iterative solution of the diffusion equation $dC/dt = D_D d^2C/dx^2$. An upper-bound

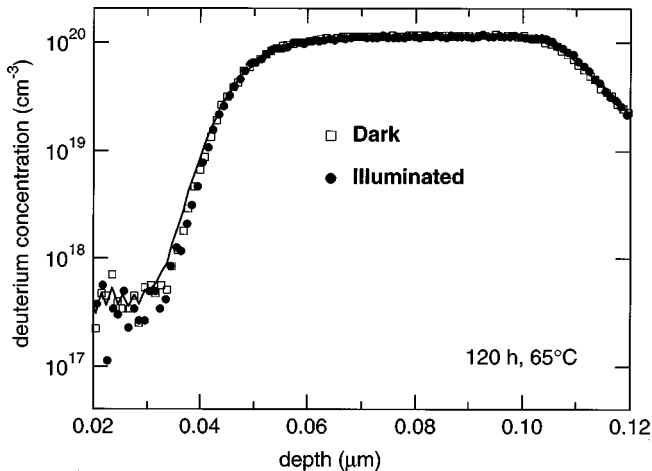


FIG. 3. D depth profiles from dark and laser-illuminated areas of a sandwich sample after 120 h at 65 °C. The solid curve is a calculated profile for diffusion with $D_D = 6 \times 10^{-20} \text{ cm}^2 \text{ s}^{-1}$.

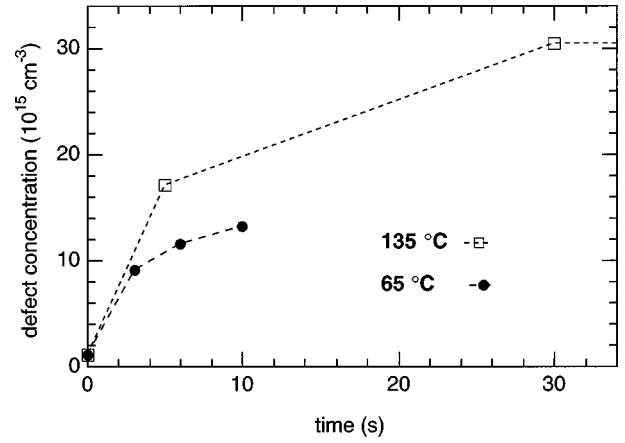


FIG. 4. CPM-absorption DB density during the early stages of nominal 65 and 135 °C illumination at the same laser intensity as used for the D tracer diffusion experiments. Dashed curves are guides to the eye.

curve for $D_D = 6 \times 10^{-20} \text{ cm}^2 \text{ s}^{-1}$ is shown in Fig. 3. It is clear that we are not seeing this amount of D diffusion. Through careful study of many measured profiles we place an upper bound of $3 \times 10^{-20} \text{ cm}^2 \text{ s}^{-1}$ on the light-induced D diffusion at 65 °C. This corresponds to a detection limit of 11 Å in the broadening of $C(x)$, a limit consistent with our studies of data reproducibility (Sec. II A).

At 300 °C, both dark and light-enhanced diffusion were easily observed. The illuminated D profile is fit very well by Eq. (1) with $D_D = 6 \times 10^{-16} \text{ cm}^2 \text{ s}^{-1}$. The dark profile was fit rather poorly by an erfc with $D_D = 4 \times 10^{-16} \text{ cm}^2 \text{ s}^{-1}$. A better fit was obtained from Eq. (2) with $\lambda_m = 110 \text{ \AA}$.

Figure 4 shows the rise of the room-temperature CPM defect density during the early stages of nominal 65 and 135 °C light soaks. It should be recalled that the temperature was actually ramped through the nominal temperature during these measurements (see Sec. II C).

IV. DISCUSSION

A. Measured light-induced D motion

Figure 5 shows an Arrhenius plot of the long-time diffusion coefficients we obtained under 9 W cm^{-2} of red illumination. For comparison, we also reproduce the data of Santos, Johnson, and Street⁷ for D tracer diffusion under 17 W cm^{-2} water-filtered white light from a xenon arc lamp. From the close agreement of the data of Santos, Johnson, and Street,⁷ and our own measurement taken at 300 °C, it appears that nearly equal light intensities reach the deuterated layer in each experiment. Our 135 °C data extend the range of the measurements to a temperature at which dark diffusion cannot be measured. Here, the D diffusion is light induced, rather than light enhanced. The activation energy of $0.9 \pm 0.1 \text{ eV}$ obtained by Santos, Johnson, and Street⁷ is valid down to at least 135 °C, supporting a phonon-assisted diffusion mechanism. Our 65 °C upper bound is consistent with an activated phonon assist down to room temperature. Our sensitivity is about an order of magnitude too low to observe the extrapolated value $D_D(65 \text{ °C}) = 4 \times 10^{-21} \text{ cm}^2 \text{ s}^{-1}$. However, with $\sim 1.5 \text{ eV}$ available from each electron-hole pair recombination, phonon-free H diffusion should become im-

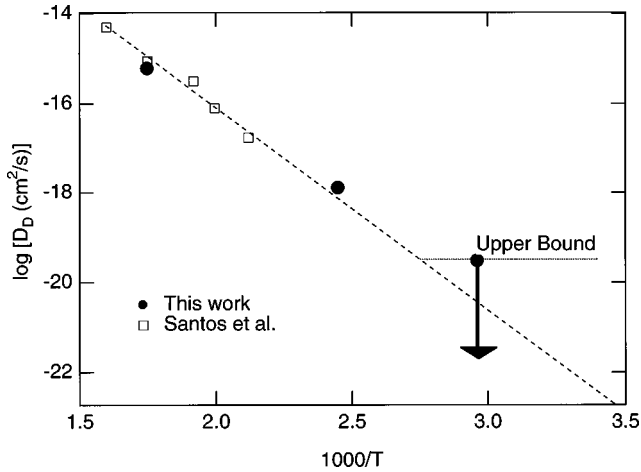


FIG. 5. Arrhenius plot of D_D during our laser illumination and during white-light soaking by Santos, Johnson, and Street (Ref. 7). Our 65 °C point is an upper bound, as indicated by the arrow. The dashed line is the best fit with 0.9±0.1 eV through the data of Ref. 7. The horizontal dotted line is an alternative extrapolation to lower temperature (see text).

portant below some critical temperature. Our 65 °C upper bound to D_D is consistent with domination of diffusion by such a temperature-independent, carrier-driven, diffusion mechanism below about 90 °C. This scenario is indicated schematically by the horizontal dotted line in Fig. 5. Plausible D tracer diffusion coefficients below 90 °C are bounded by the dotted and dashed lines.

The 10-h soak at 135 °C (Fig. 2) is in the intermediate-time regime of the diffusion in which the D emission time τ is comparable to the anneal time. We, therefore, follow the procedure described by Kemp and Branz¹⁹ to compute τ and the mean distance for D retrapping λ . Fitting the upper D wing to Eq. (2), we find for the illuminated profile that the wing amplitude B is 30–50% of the D concentration in the α -Si:H:D layer, a clear confirmation of the intermediate time regime.¹⁹ B is derived from the point at which the illuminated fit curve meets the dark profile. A small intermediate-time correction¹⁹ then yields $\tau=8\pm 2$ h and a small correction to λ_m gives a D retrapping length of $\lambda=30\pm 5$ Å. From the 10 h data, we can thus estimate $D_D=\lambda^2/\tau=(3\pm 2)\times 10^{-18}$ cm² s⁻¹, in good agreement with the long-time (100 h) value of $D_D=1.3\times 10^{-18}$ cm² s⁻¹. Our failure to see light-enhanced diffusion in 2 h at 135 °C is understood in light of

these results; the anneal time is only 0.2–0.4 of τ , while λ barely exceeds the 27 ± 3 Å exponential broadening of our unannealed profile.

The value $\lambda=30\pm 5$ Å of the D retrapping distance at 135 °C is remarkably small. Previous early time experiments by Branz *et al.*²¹ showed λ for dark D tracer diffusion rises from about 100 to 250 Å as the anneal temperature is lowered from 260 to 180 °C. These authors also obtained a value of $\lambda=50\pm 25$ Å with 380 mW/cm² of red-light illumination at 210 °C, first suggesting a reduction of λ under illumination. The observed reduction in λ and the observed increase in the D emission rate, together account for the more perfect erfc fits observed for diffusion during illumination.¹⁶

B. Light-induced H emission rates

Numerous microscopic models of light-induced metastability in α -Si:H postulate that DB's are produced when trapped H is emitted from its Si-H bond to a transport level under the influence of photoinduced carriers or their recombination.^{5–11} In these models, the light-induced motion of H (and D) should be measurable in long-range diffusion experiments. To test the models quantitatively, we first estimate the light-induced D emission rate from our tracer measurement of light-induced D diffusion. These emission rates will be compared to SW defect creation rates in Sec. IV D in order to restrict possible SW models.

D-for-H exchange^{22,23} between trapped Si-H isotopes and mobile H isotopes cannot be a step in metastable defect creation, but it greatly complicates calculation of the D emission rate. Kemp and Branz²⁴ found that symmetric D-for-H exchange (the exchange rate constants do not depend upon which isotope is mobile and which is bound) increases the measured rates of both D emission and retrapping, but leaves the measured D_D unchanged.

It is unclear whether our observed decrease of λ under illumination results from “true” light-enhanced mobile D retrapping or merely from light-enhanced exchange between mobile D and bound H. If the decrease of λ is caused by a true (nonexchange) trapping event that reduces the density of mobile H isotopes, then the high density of photogenerated carriers has sharply increased both trapping and emission of D from Si-D. However, if the light-induced decrease of λ is caused by increased D-for-H exchange, exchange emission of D likely dominates the observed D emission rate and

TABLE I. Measured D tracer diffusion coefficient and calculated light-induced D emission rates at 135 °C. λ_t is the “true” (nonexchange) trapping distance of H used to calculate ν_D . The two sets of assumptions yield upper and lower bounds to ν_D and k_D . The last column tabulates consistency with ν_{sw} from Table III and Eq. (10).

D_D (135 °C) (cm ² s ⁻¹)	Calculation assumptions		λ_t (Å)	ν_D (s ⁻¹)	k_D (cm ⁻³)	Consistent with $\nu_D \geq \nu_{sw}$
	Exchange	H retrapping				
1.3×10^{-18}	No	to unknown site	30 measured	3.5×10^{-5} measured	3.5×10^{-28}	Yes
	Yes	to DB	$850 = (6a_{db})^{-1/2}$	2×10^{-8}	2×10^{-31}	No

TABLE II. Measured upper bound to the D tracer diffusion coefficient and calculated upper bounds to light-induced D emission rates at 65 °C. λ_t is the “true” (nonexchange) trapping distance of H used to calculate ν_D . The three assumptions about the H trapping length yield different upper bounds to ν_D and k_D . The last column tabulates consistency with ν_{SW} from Table III and Eq. (10).

D_D (65 °C) ($\text{cm}^2 \text{s}^{-1}$)	Assumption: H trapping	λ_t (Å)	ν_D (s^{-1})	k_D (cm^3)	Consistent with $\nu_D \geq \nu_{SW}$
Below 3×10^{-20}	At nearest Si-Si	a	Below 6×10^{-5}	Below 3×10^{-28}	Yes
	Same as 135 °C, no exchange	30	Below 3×10^{-7}	Below 1.5×10^{-30}	Yes
	To DB	600= $(6aN_{db})^{-1/2}$	Below 8×10^{-10}	Below 8×10^{-33}	No

early- or intermediate-time profiles shed no light on the true D emission rate ν_D . We consider both possibilities explicitly, below.

Table I contains the measured value of D_D and estimates of ν_D , the true light-induced rate of D emission from Si-D to transport, derived from our 135 °C data. Because we cannot determine whether isotope exchange dominates the measured D diffusion profiles, we tabulate limiting values under two sets of assumptions.

We first assume there is no significant D-for-H exchange under illumination at 135 °C to derive an upper bound to ν_D . Then the rate of D emission is simply that observed in the 10-h light soak;

$$\nu_D = 1/\tau, \quad (3)$$

or about $3.5 \times 10^{-5} \text{ s}^{-1}$. Certainly, a light-induced increase of the true emission rate was suggested by light-enhanced D evolution from *a*-Si:D:F of Weil, Busso, and Beyer,¹⁵ in which exchange can play no role.

For a lower bound to ν_D , we assume instead that exchange dominates the early-time shape of the profiles and the observed D emission. In this case, we must rely upon the long-time measurement of D_D and estimate the true rate ν_D by assuming that DB defects are the principal traps for mobile D. Then, the nonexchange retrapping length²⁴ of D is $\lambda_t^2 = 1/6aN_{db}$, and with the microscopic definition²⁴

$$\nu_D = D_D/\lambda_t^2, \quad (4)$$

we obtain the D emission rate

$$\nu_D = D_D 6aN_{db}. \quad (5)$$

Here, a is the Si-Si interatomic distance, approximately $2.3 \times 10^{-8} \text{ cm}$. Equation (5) shows that for a particular measured value of D_D , an assumed increase in N_{db} will increase ν_D in proportion to N_{db} (by reducing λ_t). The smallest reasonable estimate of N_{db} is the saturated density of neutral DB's that can be measured once the very early stage of the light soak is complete. Hata, Isomura, and Wagner²⁵ studied the saturation of N_{db} in the same light-soaking apparatus under similar conditions and found a saturated DB density of about 10^{17} cm^{-3} . Substitution of D_D and N_{db} in Eq. (5) then yields the lower bound $\nu_D = 2 \times 10^{-8} \text{ s}^{-1}$.

These two estimates of ν_D in Table I represent upper and lower bounds that bracket most other assumptions one can

make. Intermediate assumptions include the possibility that exchange is not symmetric (D is more likely to be immobilized in the exchange process) or that D trapping to a higher density of DB's is important. These sites could be photoinduced DB's created by emission of mobile H (as suggested by the H collision model¹⁰) or charged DB's (Ref. 26) hidden from optical spectroscopy by bandtail levels.

Table II contains our measured upper bound to D_D and estimated upper bounds to ν_D at 65 °C. At 65 °C, we saw no diffusion and use only estimates of the true retrapping distances λ_t to compute upper bounds to ν_D through Eq. (4). The upper bound to D_D and an absolute lower bound on the retrapping distance of $\lambda_t > a$ (the Si-Si distance) yield the loosest upper bound on the D emission rate through Eq. (4), $\nu_D < 6 \times 10^{-5} \text{ s}^{-1}$. Assuming instead that D traps at the measured 135 °C distance of $\lambda_t = 30 \text{ Å}$, Eq. (4) yields a stricter bound of $\nu_D < 3 \times 10^{-7} \text{ s}^{-1}$. If we assume that D traps only to the neutral DB's at their saturated SW density of $2 \times 10^{17} \text{ cm}^{-3}$,²⁷ Eq. (5) gives the strictest reasonable bound of $\nu_D < 8 \times 10^{-10} \text{ s}^{-1}$.

The H collision model of light-induced metastability¹⁰ assumes H emission is proportional to the electron-hole pair generation rate G , with an emission constant $k_H = \nu_H/G$. Here, ν_H is the rate of H emission from Si-H to transport. The constant $k_D = \nu_D/G$ is found in Tables I and II. k_D is central to quantitative analysis of the H collision model of metastability under the assumption that $\nu_H = \nu_D$ and consequently $k_H = k_D$.

However, it is certainly possible that light-induced H emission may be considerably more rapid than the light-induced D emission we have measured ($\nu_H > \nu_D$). For example, hot-electron desorption of H from the Si/SiO₂ interface of metal-oxide silicon transistors appears to be 10–50 times more rapid than is desorption of D.²⁸ If this hot-carrier desorption is similar to light-induced H excitation in *a*-Si:H, light-induced emission rates of H are underestimated by our work. We plan further experiments to investigate this possibility. Obviously, it is ν_H , not ν_D , that would be relevant to SW defect creation in *a*-Si:H.

C. Defect creation rates and H emission

The key step of trap-controlled H diffusion in *a*-Si:H is emission of mobile H (H_m) from a Si-H bond to a transport level at which diffusion is quite rapid.¹⁶ Under the assumption that this emission (e.g., Si-H → DB + H_m) is always a step in metastable defect creation, as in the long-range H

TABLE III. H emission rates corresponding to defect creation and annealing during illumination. The rate $\nu_{\text{SW}}(0)$ is calculated from the initial rise of the CPM DB density. The rate ν_{SW} is calculated from the DB creation rate at saturation and represents an average value during the 10- and 100-h light soaks.

	$\nu_{\text{SW}}(0)$ (s^{-1})	ν_{SW} (s^{-1})
135 °C	6×10^{-7}	$\sim 1 \times 10^{-7}$
65 °C	5×10^{-7}	3×10^{-8}

diffusion models of the SW effect,^{5–11} we can convert light-induced DB creation rates into H emission rates. To determine the emission rate per H atom, we divide the DB rates by $N_{\text{H}} \sim 5 \times 10^{21} \text{ cm}^{-3}$. In Sec. IV D we will compare these values with D emission rates determined in Sec. IV B in order to restrict possible SW models.

The first column of Table III tabulates

$$\nu_{\text{SW}}(0) = (dN_{db}/dt)_{t=0}(1/N_{\text{H}}), \quad (6)$$

the H emission rate estimated from the earliest-time increase of DB defect density in the experiment shown in Fig. 4. DB annealing can be ignored at these early times. It should be recalled that the film temperature was actually ramping up during this early stage of light soaking (see Sec. II C).

Because of the D diffusion experiment measures the average rate of D emission to transport during our long diffusion experiments, the high *initial* $\nu_{\text{SW}}(0)$ is not the most relevant H emission rate. At a temperature between 50 and 70 °C, and an electron-hole pair generation rate of about $3 \times 10^{22} \text{ cm}^{-3} \text{ s}^{-1}$, N_{db} saturates within 1 h;²⁷ this saturation should be even more rapid at our higher intensity and temperature. Thus, the lower *average* H emission rate ν_{SW} is approximately equal to the sustained rate of defect creation at saturation and should be most relevant to our long-time diffusion experiment. We have confirmed this hypothesis by integrating the Stutzmann, Jackson, and Tsai (SJT) DB-creation rate equation,²⁹

$$dN_{db}/dt = C_{\text{SW}}G^2/N_{db}^2, \quad (7)$$

an expression that can be derived from two different theories.^{10,29} Here, C_{SW} is a constant that is measured under conditions at which light-induced annealing is unimportant. Integration of Eq. (7), including saturation of the DB density at $N_{db} = N_{\text{sat}}$ due to light-induced annealing, shows that the early period of rapid DB creation is brief and can be neglected. For our 10- and 100-h light soaks, we can, therefore, substitute $N_{db} = N_{\text{sat}}$ into Eq. (7) to obtain the average rate of DB creation,

$$dN_{db}/dt = C_{\text{SW}}G^2/N_{\text{sat}}^2. \quad (8)$$

To calculate ν_{SW} , we therefore assume that defect creation and annealing at saturation are equal and that the defect creation rate obeys Eq. (7). If SW defect creation is associated with H emission, it is reasonable to assume also that light-induced annealing must involve H emission to transport as a step in the SW DB creation. Introducing a factor of 2 into Eq. (8) to include both creation and annealing events, we obtain

$$\nu_{\text{SW}} = 2C_{\text{SW}}G^2/N_{\text{sat}}^2N_{\text{H}} \quad (9)$$

for the rate per H atom. Isomura *et al.*²⁷ measured the early time rise and the saturation of N_{db} in the same light-soaking apparatus we use and under similar conditions. At 50 to 70 °C, these authors found $C_{\text{SW}} = 300 \text{ s cm}^{-3}$ and $N_{\text{sat}} = 2 \times 10^{17} \text{ cm}^{-3}$. Substitution in Eq. (9) yields $\nu_{\text{SW}} = 3 \times 10^{-8} \text{ s}^{-1}$, corresponding to a total density of $3 \times 10^{19} \text{ cm}^{-3}$ DB's created and annealed during our 100-h soak. At 135 °C, the same authors²⁷ measured a slightly lower value $N_{\text{sat}} = 10^{17} \text{ cm}^{-3}$. There is no estimate of C_{SW} (135 °C) in the literature, so we assume C_{SW} (135 °C) = 300 s cm^{-3} , as at 65 °C. Substitution of these values in Eq. (9) then yields ν_{SW} (135 °C) $\approx 10^{-7} \text{ s}^{-1}$. This value of C_{SW} is near the upper limit of all measured values, so it represents an unfavorable assumption for the H emission models of metastability. The estimates of ν_{SW} at 65 and 135 °C are found in Table III and are used in the following section to quantitatively test the mutual compatibility of SW effect and D diffusion models.

D. Comparison of emission rates

To test quantitatively the models of SW metastability in which DB creation is accompanied by emission of H to transport,^{5–11} we must compare the various emission rates found in Tables I–III. In principle, viability of these models requires simply that

$$\nu_{\text{D}} \geq \nu_{\text{SW}}, \quad (10)$$

i.e., the emission rate of D observed in diffusion (and assumed equal to that of H) must be greater than or equal to that deduced from the rise of N_{db} during light soaking. In practice, this comparison of ν_{D} and ν_{SW} is more complicated. As described in Sec. IV B, many assumptions about D tracer diffusion and its relation to H emission rates underlie the values of ν_{D} found in Tables I and II. Further, there is uncertainty in the estimates of ν_{SW} in Table III. Still, the range of viable SW and light-induced diffusion models can be restricted using our data.

We first note that there is a rough consistency to the orders of magnitude of ν_{D} and ν_{SW} measured in our experiments. Given the uncertainties in our estimates of both quantities, the data as a whole certainly appear to be consistent with H emission models of the SW effect. A careful examination of particular models does reveal that only certain assumptions about H retrapping during light-induced diffusion are compatible with the long-range H diffusion models of the SW effect, as tabulated in the final columns of Tables I and II.

At 135 °C, we compare the data of Tables I and III for consistency with Eq. (10). If we assume that the measured D emission rate is identical to the H emission rate (and not dominated by an H-for-D exchange process), then we must compare ν_{D} (135 °C) from the top row of Table I to ν_{SW} (135 °C) from Table III. Since $3.5 \times 10^{-5} \text{ s}^{-1} \gg 10^{-7} \text{ s}^{-1}$, H emission models of SW are certainly consistent with our data, as indicated in Table I. However, H-emission models are narrowly excluded if we assume that exchange dominates D tracer emission and D retrapping in only to Staebler-Wronski DB's at their saturation density. In this case, we

must compare ν_D (135 °C) from the bottom row of Table I to ν_{SW} (135 °C) from Table III. Since $10^{-7} \text{ s}^{-1} \gg 2 \times 10^{-8} \text{ s}^{-1}$, the diffusion-derived H emission rate is too low to explain the measured rise of DB density. However, the H emission models are viable even with exchange if we assume that during high-intensity light soaking there are H retrapping sites at a density above about 10^{18} cm^{-3} . In this case ν_D (135 °C) is calculated using Eq. (5) and again compared to ν_{SW} (135 °C) through Eq. (10).

As we find no 65 °C D tracer diffusion, our 65 °C data cannot be used to support H emission models of the metastability—in any sense. However, we can check whether the long-range H diffusion models of the SW effect are consistent with our data by comparing the data of Tables II and III. If we assume λ_t (65 °C) equal to the measured higher-temperature value of λ (135 °C) = 30 Å, we must compare ν_D (65 °C) from the middle row of Table II to ν_{SW} (65 °C) from Table III. Since $3 \times 10^{-7} \text{ s}^{-1} \gg 3 \times 10^{-8} \text{ s}^{-1}$, Eq. (10) implies that H emission models of the SW effect are consistent with our data, as indicated in Table II. The same conclusion holds for shorter retrapping lengths. From Eq. (4), we find that the range of retrapping lengths consistent with Eq. (10) is $\lambda_t \leq 100$ Å. Through Eq. (5), this corresponds to a D-trapping site density greater than about $4 \times 10^{18} \text{ cm}^{-3}$. For $\lambda_t > 100$ Å (i.e., lower H-trapping site densities), the SW models are inconsistent with our data. For example, retrapping to SW DB's at the measured saturated density ($2 \times 10^{17} \text{ cm}^{-3}$) is tested by comparing ν_D (65 °C) from the bottom row of Table II to ν_{SW} (65 °C) from Table III. This assumption yields $\lambda_t = 600$ Å, and since $8 \times 10^{-10} \text{ s}^{-1} \ll 3 \times 10^{-8} \text{ s}^{-1}$, it renders the long-range H diffusion models inconsistent with our diffusion data.

V. CONCLUSIONS

We measure light-induced D tracer diffusion at 135 °C, a temperature so low that thermal diffusion is not observable.

The data confirm and extend to lower T the previously observed 0.9 eV activation energy of light-induced diffusion. Early time measurements at 135 °C also yield $\lambda = 30 \pm 5$ Å, showing that light reduces the D retrapping distance dramatically. Estimates of the light-induced D emission rate from Si-H bonds are obtained. At 65 °C, no light-induced diffusion was observed, but upper bounds to the light-induced emission rate of mobile D are obtained.

SW models requiring emission of mobile H from Si-H to a transport level⁵⁻¹¹ are consistent with our diffusion data and our CPM data for the light-induced creation of DB defects, under the assumption that excited mobile D tracer atoms retrap to a density of sites greater than about 10^{18} cm^{-3} . For example, D could retrap to a high density of transient DB's present during high-intensity illumination. If it is assumed, however, that only neutral DB's remaining in the sample after light soaking can retrap D tracer atoms under high-intensity light soaking, then both our 65 and 135 °C diffusion data appear to exclude this class of SW models. However, if light-induced emission of mobile H is significantly more rapid than light-induced emission of D, SW models requiring emission of mobile H could still be viable. Further study of the D emission and retrapping mechanism under high-intensity light soaking will be necessary to draw stronger conclusions.

ACKNOWLEDGMENTS

We are extremely grateful to John Bullock for many helpful discussions of defect creation rates and to Brent Nelson for depositing the sandwich structures. Richard Crandall, Klaus Lips, and Arthur Yelon also made valuable suggestions. This work was supported in part by the U.S. DOE under Contract No. DE-AC36-83CH10093, and in part by the Amorphous Thin Film Solar Cell Program at the Electric Power Research Institute.

- ¹D. L. Staebler and C. R. Wronski, Appl. Phys. Lett. **31**, 292 (1977).
- ²D. L. Staebler and C. R. Wronski, J. Appl. Phys. **51**, 3262 (1980).
- ³M. Stutzmann, W. B. Jackson, and C. C. Tsai, Phys. Rev. B **32**, 23 (1985).
- ⁴D. E. Carlson, Appl. Phys. A: Solids Surf. **41**, 305 (1986).
- ⁵H. Dersch, J. Stuke, and J. Beichler, Appl. Phys. Lett. **38**, 456 (1981).
- ⁶S. B. Zhang, W. B. Jackson, and D. J. Chadi, Phys. Rev. Lett. **65**, 2575 (1990).
- ⁷P. V. Santos, N. M. Johnson, and R. A. Street, Phys. Rev. Lett. **67**, 2686 (1991).
- ⁸R. Prasad and S. R. Shenoy, Phys. Lett. A **218**, 85 (1996).
- ⁹C. Godet, Philos. Mag. B **77**, 765 (1998).
- ¹⁰H. M. Branz, Solid State Commun. **105**, 387 (1998); H. M. Branz, preceding paper, Phys. Rev. B **59**, 5498 (1999).
- ¹¹R. Biswas and B. C. Pan, Appl. Phys. Lett. **72**, 371 (1998).
- ¹²P. Stradins and H. Fritzsche, Philos. Mag. B **69**, 121 (1994).
- ¹³S. Yamasaki and J. Isoya, J. Non-Cryst. Solids **164-166**, 169 (1993).
- ¹⁴M. Stutzmann, in *Amorphous and Microcrystalline Silicon Technology—1997*, edited by E. A. Schiff, M. Hack, S. Wagner, R. Schropp, and I. Shimizu, MRS Symposia Proceedings No. 467 (Materials Research Society, Pittsburgh, 1997), p. 37.
- ¹⁵R. Weil, A. Busso, and W. Beyer, Appl. Phys. Lett. **53**, 2477 (1988).
- ¹⁶H. M. Branz, S. E. Asher, and B. P. Nelson, Phys. Rev. B **47**, 7061 (1993).
- ¹⁷O. Greim, J. Weber, Y. Baer, and U. Kroll, Phys. Rev. B **50**, 10 644 (1994).
- ¹⁸P. V. Santos and N. M. Johnson, Appl. Phys. Lett. **62**, 720 (1993).
- ¹⁹M. Kemp and H. M. Branz, Phys. Rev. B **47**, 7067 (1993).
- ²⁰Z. Smith, Ph.D. thesis, Princeton University, 1987.
- ²¹H. M. Branz, S. E. Asher, B. P. Nelson, and M. Kemp, in *Amorphous Silicon Technology—1993*, edited by E. A. Schiff, A. Madan, M. J. Thompson, K. Tanaka and P. G. LeComber, MRS Symposia Proceedings No. 297 (Materials Research Society, Pittsburgh, 1993), p. 279.
- ²²B. Abeles, L. Yang, D. P. Leta, and C. Majkrzak, in *Interfaces, Superlattices and Thin Films*, edited by J. D. Dow and I. K.

- Schuller, MRS Symposia Proceedings No. 77 (Materials Research Society, Pittsburgh, 1987), p. 623.
- ²³H. M. Branz, S. E. Asher, Y. Xu, and M. Kemp, in *Amorphous Silicon Technology—1995*, edited by M. Hack, E. A. Schiff, A. Madan, M. Powell, and A. Matsuda, MRS Symposia Proceedings No. 377 (Materials Research Society, Pittsburgh, 1995), p. 331.
- ²⁴M. Kemp and H. M. Branz, Phys. Rev. B **52**, 13 946 (1995).
- ²⁵N. Hata, M. Isomura, and S. Wagner, Appl. Phys. Lett. **60**, 1462 (1992).
- ²⁶H. M. Branz and M. Silver, Phys. Rev. B **42**, 7420 (1990).
- ²⁷M. Isomura, H. R. Park, N. Hata, A. Maruyama, P. Roca i Cabarocas, S. Wagner, J. R. Abelson, and F. Finger, in *Proceedings of the International PVSEC-5*, edited by H. Umeno and H. Matsumami (International PVSEC-5, Kyoto, Japan, 1990), p. 71.
- ²⁸J. W. Lyding, K. Hess, and I. C. Kizilyalli, Appl. Phys. Lett. **68**, 2526 (1996).
- ²⁹M. Stutzmann, W. B. Jackson, and C. C. Tsai, Appl. Phys. Lett. **45**, 1075 (1984).